Proceedings of ASME 2013 International Mechanical Engineering Congress & Exposition
IMECE 2013
November 13-21, 2013, San Diego, USA

IMECE2013-63751

DRAFT: STABILITY ANALYSIS FOR A FORCE AUGMENTING DEVICE CONSIDERING DELAYS IN THE HUMAN MODEL

Suresh K. Gadi
Department of Automatic Control
UMI LAFMIA CNRS-CINVESTAV
Av. IPN 2508. Mexico City, 07360, Mexico
sgadi@ctrl.cinvestav.mx

Ruben A. Garrido *
Department of Automatic Control
UMI LAFMIA CNRS-CINVESTAV
Av. IPN 2508. Mexico City, 07360, Mexico
garrido@ctrl.cinvestav.mx

Rogelio Lozano
Heudiasyc UMR-7253, CNRS-UTC
Compiegne, France
rogelio.lozano@hds.utc.fr

Antonio Osorio
CGSTIC, CINVESTAV
Av. IPN 2508. Mexico City, 07360, Mexico
aosorio@cinvestav.mx

ABSTRACT

This paper presents a stability analysis of the interaction between a human and a linear moving Force Augmenting Device (FAD). The analysis employs the mathematical models of the human, the FAD and their interaction. As a depart from past works, this article presents a stability analysis considering time-delays in the human model. A key ingredient in the analysis is the use of the Rekasius substitution for replacing the time-delay terms. It is proved that the human machine interaction is stable when the human model has no delays. The analysis provides an upper bound for the time-delays preserving a stable interaction. Numerical simulations allow to assess the human-FAD interaction. An experiment is performed with a laboratory prototype, where a human operator lifts a load. It is observed that the human machine interaction is stable and the human operator is able to move the load to its desired position by experiencing very little effort.

*Address all correspondence to this author.

NOMENCLATURE

θ_h Human arm position
θ_{vd} Virtual desired position
θ_v Output of the spinal cords reflex action
τ_h External torque acting on the human joint
B Viscous friction in the human arm movement
d_1 Delay in the position reflex feedback
d_2 Delay in the velocity reflex feedback
E Physical compliance of the human flesh
F Total force exerted on the moving block
F_A Force exerted by the motor on the moving block
F_e Force exerted by the human on the moving block
F_h Force exerted by the moving block on the human arm
g Acceleration due to gravity
G_p Control parameter of the spinal chord
G_v Control parameter of the spinal chord
J Human arm moment of inertia
K Muscle stiffness
K_A Force augmenting gain
K_d Derivative gain
K_f Viscous friction coefficient of FAD
K_p Proportional gain
l_a Human arm length

M Mass of the moving block
s Laplace transform complex variable
t Time
W Weight of the moving block
y_h Human arm displacement at the end of the arm

INTRODUCTION

Recently, there has been a lot of interest in developing exoskeletons and force augmenting devices [1], i.e. mechanical systems that are worn by humans in such a way as to increase their force. There exist many possible applications for these devices; for instance, in industries where it is commonly required to move heavy loads. This task is mostly done by machines, which are usually controlled by humans who do not necessarily feel the force exerted on the load. This may lead to unsafe operations in confined spaces with obstacles. Exoskeletons and force augmenting devices (FAD) represent a possible solution to this problem [2]. Indeed a FAD amplifies the human strength and allows the operator handling heavy loads but still feeling the effort performed to move the load [3].

There are many papers in the literature dealing with human-machine interaction [4–10], however the stability of the proposed control algorithms has not been thoroughly studied. In order to study the stability of the human machine interaction we need to introduce a model for the human behaviour. There are several possible models for the human operator [11–15] and we have selected the model proposed in [12] because it takes into account the delays present in the human reflexes.

In this paper we present a simple controller for the FAD and a stability proof of its interaction with a human operator. We first study the stability of the interaction considering no delays in the human model. The closed loop system is of 4th order and the proof of the stability is carried out using the Routh-Hurwitz stability criterion. Furthermore, we have also studied the stability considering delays in the human model. An upper bound for the delays has been found such that the stability is preserved. The human-FAD interaction is illustrated through numerical simulations.

The paper is organized as follows: The next section introduces a model of the FAD, a model of a human operator and the control algorithm proposed in [16] for the FAD. This is followed by a section providing the stability proof for the system ignoring delays in the human model. Subsequently, the stability is studied considering that both delays in the human model are equal. In the next section a stability analysis is performed assuming that both delays in the human model are independent. Simulation and experimental results support the results obtained. Concluding remarks are given in the final section.

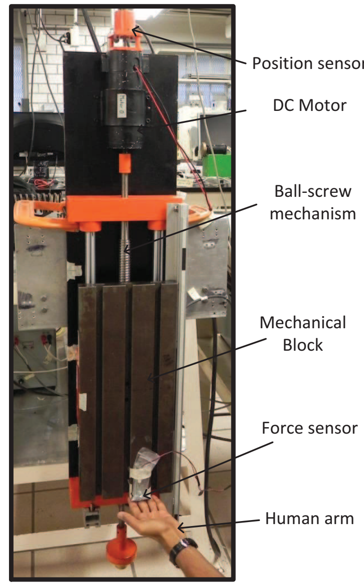

Figure 1. PHOTO OF A HUMAN OPERATING A LINEAR FORCE AUGMENTING DEVICE

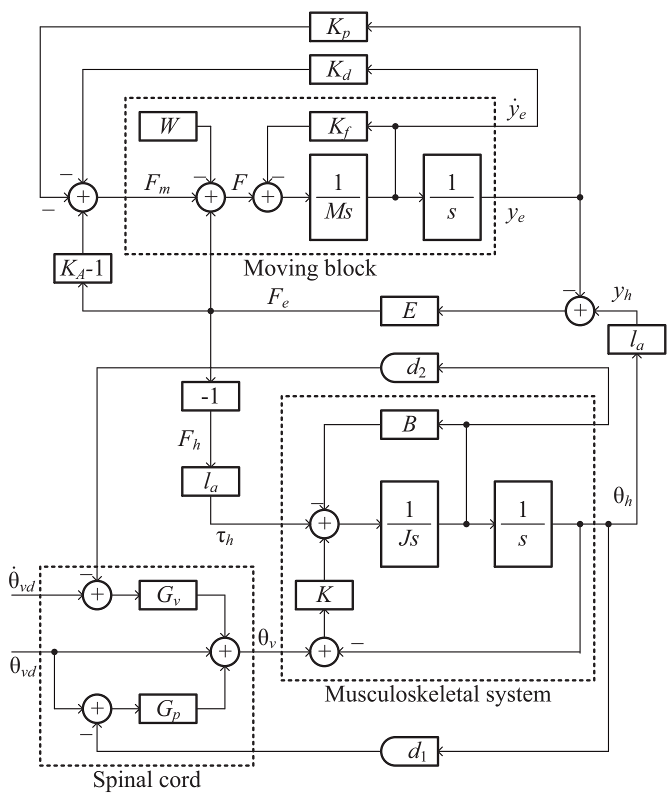

Figure 2. BLOCK DIAGRAM OF THE HUMAN-FAD INTERACTION

MATHEMATICAL MODEL

The force augmenting device (FAD) considered in this paper is shown in Fig. 1 and Fig. 2 depicts its block diagram. This figure also shows the interaction between a human operator and the FAD. The FAD has a moving block of 24 kg connected to a ball-screw mechanism, and acts as the load to be lifted by the human operator. The ball-screw mechanism is driven by a DC servo motor. Force and position sensors are attached to the FAD to capture the force exerted by the human on the moving block and to measure its position respectively. The total force exerted on the moving block (F) can be decomposed as

$$F = F_A + F_e - W \tag{1}$$

where $W = Mg$. Considering zero initial conditions, the dynamics of the moving block can be written as

$$\frac{y_e(s)}{F(s)} = \frac{1}{Ms^2 + K_f s} \tag{2}$$

The human model used for describing the human operator arm is based on a servo hypothesis proposed in [12], where the spinal cord actuates the muscles of the musculoskeletal system by computing the signals received from the brain, and the position and velocity feedback signals produced by the sensory organs of the musculoskeletal system. The position reached by the human arm is not exactly equal to the position commanded by the spinal cord due to the arm inertia, so the command given by the spinal cord to the musculoskeletal system is termed as the virtual position [12,17]. The human brain generates a desired trajectory through which the arm must move; based on the desired trajectory the brain computes a signal and sends it to the spinal cord [13], which is the virtual desired position [12]. The musculoskeletal system is modeled as a second order linear transfer function.

The dynamics of the musculoskeletal system shown in Fig. 2 can be written as

$$\tau_h(s) = J\ddot{\theta}_h(s) + B\dot{\theta}_h(s) + K(\theta_h(s) - \theta_v(s)) \tag{3}$$

The term θ_v represents the virtual arm position. In a human being, the sensory feedback received by the spinal cord is delayed. This delay makes the stability issue challenging. The following equation represents the spinal cord reflex action:

$$\begin{aligned}\theta_v(s) = {} & \theta_{vd}(s) + G_p(\theta_{vd}(s) - \theta_h(s)e^{-sd_1}) + sG_v(\theta_{vd}(s) \\ & -\theta_h(s)e^{-sd_2})\end{aligned} \tag{4}$$

The force exerted by the human arm F_e on the moving block can be expressed as

$$F_e(t) = -F_h(t) = (y_h(t) - y_e(t))E \tag{5}$$

$$y_h(t) = \theta_h(t) l_a \tag{6}$$

The torque exerted by the moving block on the human arm can be given as

$$\tau_h(t) = F_h(t) l_a = (y_e(t) - y_h(t))El_a \tag{7}$$

The following control algorithm [16] is applied to the FAD:

$$F_A(t) = (K_A - 1)F_e(t) - K_d\dot{y}_e(t) - K_p y_e(t) \tag{8}$$

where K_A is the augmenting factor which allows amplifying the force exerted by the human operator and the term $K_d\dot{y}_e(t)$ introduces the required damping into the system.

Since the input terms W, y_{vd} and sy_{vd} do not affect the stability, these terms can be neglected for the stability study. The characteristic equation for the closed loop system can be written as

$$P(s) = C_4 s^4 + C_3 s^3 + C_2 s^2 + C_1 s + C_0 \tag{9}$$

where

$$C_4 = JM \tag{10}$$

$$C_3 = M(B + G_v K e^{-sd_2}) + J(K_d + K_f) \tag{11}$$

$$\begin{aligned}C_2 = {} & M(El_a^2 + K(G_p e^{-sd_1} + 1)) + (K_d + K_f)(B \\ & + G_v K e^{-sd_2}) + J(K_p + EK_A)\end{aligned} \tag{12}$$

$$\begin{aligned}C_1 = {} & (B + G_v K e^{-sd_2})(K_p + EK_A) + (K_d + K_f)(El_a^2 \\ & + K(G_p e^{-sd_1} + 1))\end{aligned} \tag{13}$$

$$C_0 = (K_p + EK_A)(El_a^2 + K(G_p e^{-sd_1} + 1)) - E^2 K_A l_a^2 \tag{14}$$

In the following section we will study the stability of the above polynomial.

STABILITY ANALYSIS WHEN THE DELAYS ARE ZERO

Considering that $d_1 = d_2 = 0$, equation (9) can be rewritten as

$$P(s) = A_4 s^4 + A_3 s^3 + A_2 s^2 + A_1 s + A_0 \tag{15}$$

where

$$A_4 = JM \quad (16)$$
$$A_3 = M(B+G_vK)+J(K_d+K_f) \quad (17)$$
$$A_2 = M(El_a^2+K(G_p+1))+(K_d+K_f)(B+G_vK) +J(K_p+EK_A) \quad (18)$$
$$A_1 = (B+G_vK)(K_p+EK_A)+(K_d+K_f)(El_a^2+K(G_p +1)) \quad (19)$$
$$A_0 = EK_pl_a^2+(G_p+1)KK_p+E(G_p+1)KK_A \quad (20)$$

As per the Routh-Hurwitz stability criterion, the closed loop system is stable if and only if

$$A_0 > 0; A_1 > 0; A_2 > 0; A_3 > 0; A_4 > 0; A_5 > 0 \quad (21)$$
$$b_1 := \big(A_3A_2-A_4A_1\big)/A_3 > 0 \quad (22)$$
$$c_1 := \big(b_1A_1-A_3A_0\big)/b_1 > 0 \quad (23)$$

See the Appendix to verify that these conditions are met indeed.

STABILITY CONSIDERING IDENTICAL DELAYS

Assume that both delays are the same, i.e. $d_1 = d_2 = d$. The substitution proposed by Rekasius is [18, 19]

$$e^{-sd} = \frac{1-Ts}{1+Ts} \qquad T\in\Re, \quad d\in\Re^+ \quad (24)$$

which is defined when $s = j\omega$, $\omega\in\Re$. This substitution allows to replace the exponential transcendental term associated to the time-delay (i.e. e^{-sd}) by a rational expression of the variables s and T. The relation between d , T and ω can be given as [18, 19]

$$d = \frac{2}{\omega}\arctan(T\omega)+l\pi \qquad l=-\infty,\dots-1,0,1,\dots,\infty \quad (25)$$

where for a fixed ω each T maps to infinitely many values of d. Substituting (24) into (9), we get

$$P(s) = B_5s^5+B_4s^4+B_3s^3+B_2s^2+B_1s+B_0 \quad (26)$$

where

$$B_5 = JMT \quad (27)$$
$$B_4 = JM+BMT+J(K_d+K_f)T-G_vKMT \quad (28)$$
$$B_3 = EMTl_a^2+BM+J(K_d+K_f)+G_vKM+B(K_d +K_f)T+JK_pT+KMT+EJK_AT-G_vK(K_d +K_f)T-G_pKMT \quad (29)$$
$$B_2 = B(K_d+K_f)+JK_p+KM+EJK_A+G_vK(K_d +K_f)+G_pKM+BK_pT+K(K_d+K_f)T+EMl_a^2 +E(K_d+K_f)Tl_a^2+BEK_AT-G_pK(K_d+K_f)T -G_vKK_pT-EG_vKK_AT \quad (30)$$
$$B_1 = BK_p+K(K_d+K_f)+BEK_A+G_pK(K_d+K_f) +G_vKK_p+KK_pT+E(K_d+K_f)l_a^2+EK_pTl_a^2 +EG_vKK_A+EKK_AT-G_pKK_pT-EG_pKK_AT \quad (31)$$
$$B_0 = EK_pl_a^2+KK_p+EKK_A+G_pKK_p+EG_pKK_A \quad (32)$$

The estimated values for the laboratory setup shown in Fig. 1 are $M = 23.4\,\mathrm{kg}$ and $K_f = 0\,\mathrm{N\,m^{-1}\,s}$. The authors in [12] use the following parameters for a human arm: $J = 0.1\,\mathrm{N\,m\,rad^{-1}\,s^{-2}}$, $B = 0.89\,\mathrm{N\,m\,rad^{-1}\,s^{-1}}$, $K = 4\,\mathrm{N\,m\,rad^{-1}}$, $G_p = 2$ and $G_v = 0.3\,\mathrm{s}$. The value $E = 920\,\mathrm{N\,m^{-1}}$ for human flesh is given in [20]. Taking $l_a = 0.35\,\mathrm{m}$ and the control parameters $K_A = 125$, $K_d = 65\,\mathrm{kg\,s^{-1}}$ and $K_p = 45\,\mathrm{kg\,s^{-2}}$. Substituting these values in $P(s)$, (26) is rewritten as

$$P(s) = 2.3\times10^5Ts^5+(2.3\times10^5-7.5\times10^4T)s^4 +(1.4\times10^9T+5.5\times10^6)s^3+(1.5\times10^9 -2.9\times10^9T)s^2+(2.5\times10^{10}-4.6\times10^{10}T)s +1.4\times10^{11} \quad (33)$$

Since the system is stable when the delays are zero, all the poles are in the left hand side of the complex plane. New poles are introduced from the left hand side of the complex plane as a consequence of the delays [21]. The position of the poles in the complex plane as a function of the delay is continuous [21, 22]. As the delays increase, the poles move towards the right hand side of the plane and finally cross the $j\omega$ axis. The substitution (24) is valid at the moment when the poles are on the imaginary axis just before crossing it.

A Routh array can be constructed for (33) as

$$\begin{array}{c|ccc}
s^5 & 2.3\times10^5T & (140.3T+0.6)\times10^6 & B_{53} \\
s^4 & (2.3-0.8T)\times10^5 & (1.5-2.9T)\times10^9 & B_{43} \\
s^3 & B_{31} & B_{32} & 0 \\
s^2 & B_{21} & 1.4\times10^{11} & 0 \\
s^1 & B_{11} & 0 & 0 \\
s^0 & 1.4\times10^{11} & 0 & 0
\end{array}$$

where

$$B_{53} = (2.5-4.6T)\times10^{10}$$

$$
\begin{aligned}
B_{43} &= 1.4\times10^{11}\\
B_{31} &= 1\times10^{8}\left(563.5T^2-12.8T+1.3\right)\Big/\left(23.4-7.5T\right)\\
B_{32} &= 5\times10^{10}\left(6.8T^2-89.9T+11.6\right)\Big/\left(23.4-7.5T\right)\\
B_{21} &= -1\times10^{8}\Big(16113.9T^3-8528.6T^2+114.2T\\
&\quad -5.3\Big)\Big/\left(563.5T^2-12.8T+1.3\right)\\
B_{11} &= -1\times10^{10}\Big(14.7T^4-37.7T^3+4.5T^2-0.07T\\
&\quad +2416.6\Big)\Big/\left(16.1T^3-8.5T^2+0.1T-0.005\right)
\end{aligned}
$$

As per the Routh-Hurwitz stability criterion, when the poles are on the imaginary axis, a row of the Routh array becomes zero and its previous row is called the auxiliary polynomial. The auxiliary polynomial gives the location of the poles on the imaginary axis. Solving $B_{11}=0$ and considering only real values for T, the solution is $T=2.44372$ or $T=0.11131$. The auxiliary polynomial (P_A) is given by the next expression

$$P_A = B_{21}s^2+1.4\times10^{11} \tag{34}$$

Solving (34) at $T=2.44372$ and $T=0.11131$, yields respectively $s=j\omega=\pm j(j5.0048)$ and $s=j\omega=\pm j11.1765$. Since $\omega\in\Re$, $T=0.11131, \omega=11.1765$ is the required value. A given $\omega\in\Re$ and $T\in\Re$ produce infinite time-delays d satisfying (25), at which a pair of poles are transferred from one side to another. Equation (25) is used to obtain the following values:

$$
\begin{aligned}
d|_{l=0} &= 0.1599\\
d|_{l=1} &= 3.3015\\
d|_{l=-1} &= -2.9817
\end{aligned}
$$

The smallest positive delay at which the poles cross the imaginary axis for the first time is called the critical delay (d_c). The critical delay for this system occurs for the values $l=0$, $d=d_c=0.1599$. Repeating the above calculations for the different values of K_A, we can obtain the critical delay corresponding to K_A. Fig. 3 shows the change in the critical delay as a function of the augmenting factor K_A.

STABILITY CONSIDERING INDEPENDENT DELAYS

In this section let us consider different delays d_1 and d_2. A Rekasius substitution similar to (24) for the two time-delays is

$$e^{-sd_1} = \frac{1-T_1s}{1+T_1s} \qquad T_1\in\Re,\quad d_1\in\Re^+ \tag{35}$$

$$e^{-sd_2} = \frac{1-T_2s}{1+T_2s} \qquad T_2\in\Re,\quad d_2\in\Re^+ \tag{36}$$

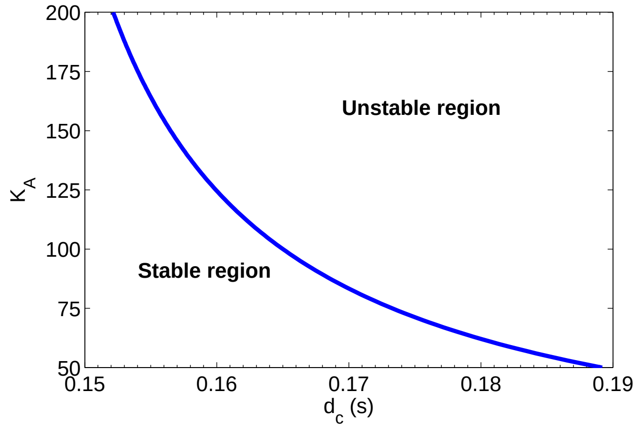

Figure 3. CRITICAL DELAY d_c AT $50\le K_A\le 200$ IN EQUAL DELAY CASE (i.e. $d_1=D_2$)

and the relation between T_1, ω_1, and d_1 and T_2, ω_2, and d_2 is given as

$$d_1 = \frac{2}{\omega}\arctan\left(T_1\omega\right)+l\pi \qquad l=-\infty,\ldots-1,0,1,\ldots,\infty \tag{37}$$

$$d_2 = \frac{2}{\omega}\arctan\left(T_2\omega\right)+l\pi \qquad l=-\infty,\ldots-1,0,1,\ldots,\infty \tag{38}$$

Substituting (35) and (36) into (9), we get

$$P(s) = D_6s^6+D_5s^5+D_4s^4+D_3s^3+D_2s^2+D_1s+D_0 \tag{39}$$

where

$$D_6 = JMT_1T_2 \tag{40}$$

$$
\begin{aligned}
D_5 &= JMT_1+JMT_2+BMT_1T_2+JK_dT_1T_2+JK_fT_1T_2\\
&\quad -G_vKMT_1T_2
\end{aligned} \tag{41}
$$

$$
\begin{aligned}
D_4 &= EMT_1T_2l_a^2+JM+BMT_1+BMT_2+JK_dT_1+JK_dT_2\\
&\quad +JK_fT_1+JK_fT_2+G_vKMT_1-G_vKMT_2+BK_dT_1T_2\\
&\quad +BK_fT_1T_2+JK_pT_1T_2+KMT_1T_2+EJK_AT_1T_2\\
&\quad -G_vKK_dT_1T_2-G_vKK_fT_1T_2-G_pKMT_1T_2
\end{aligned} \tag{42}
$$

$$
\begin{aligned}
D_3 &= BM+JK_d+JK_f+G_vKM+BK_dT_1+BK_dT_2+BK_fT_1\\
&\quad +BK_fT_2+JK_pT_1+JK_pT_2+KMT_1+KMT_2+EMT_1l_a^2\\
&\quad +EMT_2l_a^2+EJK_AT_1+EJK_AT_2+G_vKK_dT_1-G_vKK_dT_2\\
&\quad +G_vKK_fT_1-G_vKK_fT_2-G_pKMT_1+G_pKMT_2\\
&\quad +BK_pT_1T_2+KK_dT_1T_2+KK_fT_1T_2+EK_dT_1T_2l_a^2\\
&\quad +EK_fT_1T_2l_a^2+BEK_AT_1T_2-G_pKK_dT_1T_2-G_pKK_fT_1T_2\\
&\quad -G_vKK_pT_1T_2-EG_vKK_AT_1T_2
\end{aligned} \tag{43}
$$

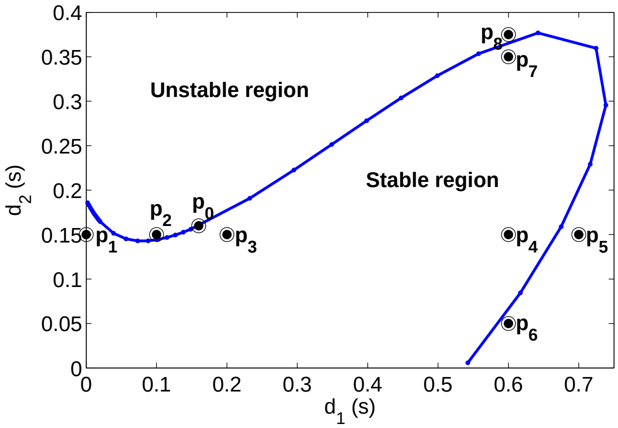

Figure 4. CRITICAL DELAYS FOR d_1 AND d_2 AT $K_A = 125$

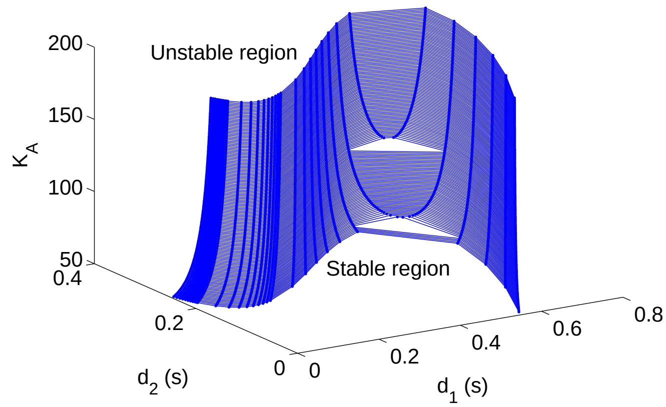

Figure 5. CRITICAL DELAYS FOR d_1 AND d_2 AT $50 \le K_A \le 200$

$$
\begin{aligned}
D_2 = {} & BK_d + BK_f + JK_p + KM + EJK_A + G_vKK_d + G_vKK_f \\
& + G_pKM + BK_pT_1 + BK_pT_2 + KK_dT_1 + KK_dT_2 + KK_fT_1 \\
& + KK_fT_2 + EMl_a^2 + EK_dT_1l_a^2 + EK_dT_2l_a^2 + EK_fT_1l_a^2 \\
& + EK_fT_2l_a^2 + BEK_AT_1 + BEK_AT_2 - G_pKK_dT_1 + G_pKK_dT_2 \\
& - G_pKK_fT_1 + G_pKK_fT_2 + G_vKK_pT_1 - G_vKK_pT_2 \\
& + KK_pT_1T_2 + EK_pT_1T_2l_a^2 + EG_vKK_AT_1 - EG_vKK_AT_2 \\
& + EKK_AT_1T_2 - G_pKK_pT_1T_2 - EG_pKK_AT_1T_2 \qquad (44)
\end{aligned}
$$

$$
\begin{aligned}
D_1 = {} & BK_p + KK_d + KK_f + BEK_A + G_pKK_d + G_pKK_f \\
& + G_vKK_p + KK_pT_1 + KK_pT_2 + EK_dl_a^2 + EK_fl_a^2 + EK_pT_1l_a^2 \\
& + EK_pT_2l_a^2 + EG_vKK_A + EKK_AT_1 + EKK_AT_2 - G_pKK_pT_1 \\
& + G_pKK_pT_2 - EG_pKK_AT_1 + EG_pKK_AT_2 \qquad (45)
\end{aligned}
$$

$$
D_0 = EK_pl_a^2 + KK_p + EKK_A + G_pKK_p + EG_pKK_A \qquad (46)
$$

Using the values for the parameters B, E, G_p, G_v, J, K, K_A, K_d, K_f, K_p, l_a, M given in the previous section, we can rewrite (39) as

$$
\begin{aligned}
P(s) = {} & T_1T_2s^6 + (T_1 + T_2 - 0.3T_1T_2)s^5 + (23.7T_1 - 0.3T_2 \\
& + 6\times10^3T_1T_2 + 1)s^4 + (6\times10^3T_1 + 6\times10^3T_2 \\
& - 1\times10^4T_1T_2 + 23.7)s^3 + (1.1\times10^5T_1 - 1.2\times10^4T_2 \\
& - 2\times10^5T_1T_2 + 6.2\times10^3)s^2 + (6\times10^5T_2 - 2\times10^5T_1 \\
& + 1.1\times10^5)s + 6\times10^5 \qquad (47)
\end{aligned}
$$

Substituting T_1 by a numerical value into (47), we get (47) with only one variable T_2, which is similar to (33). The computation for solving T given in the previous section can be used to obtain T_2, therefore the critical delays corresponding to T_1 and T_2 can be computed using (37) and (38).

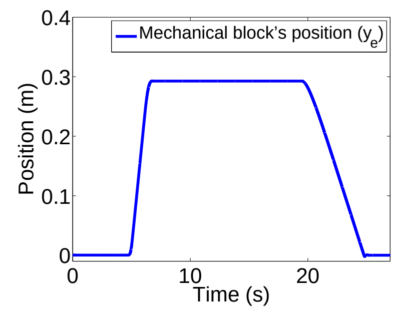

Figure 7. EXPERIMENTAL RESULT: POSITION VS TIME

Varying T_1 in the region [0.001 10] and solving for T_2 we obtain critical delays for d_1 and d_2, see Fig. 4. Also, varying K_A from 50 to 200, we obtain Fig. 5 which shows the critical delays of d_1 and d_2 as a function of K_A.

SIMULATION RESULTS

A simulation has been performed on the system shown in Fig. 2 using MATLAB Simulink. A Runge-Kutta solver of 4^{th} order with a step size of 1 ms is used for the numerical simulation. Simulation is performed with the system parameters given in the previous sections and K_A is taken as 125. Let $p = (d_1, d_2)$ be any point on Fig. 4 representing delays. Simulation is performed at $p_0 = (0.1599, 0.1599)$, $p_1 = (0, 0.15)$, $p_2 = (0.1, 0.15)$, $p_3 = (0.2, 0.15)$, $p_4 = (0.6, 0.15)$, $p_5 = (0.7, 0.15)$, $p_6 = (0.6, 0.05)$, $p_7 = (0.6, 0.35)$, $p_8 = (0.6, 0.375)$. The simulation results are shown in Fig. 6.

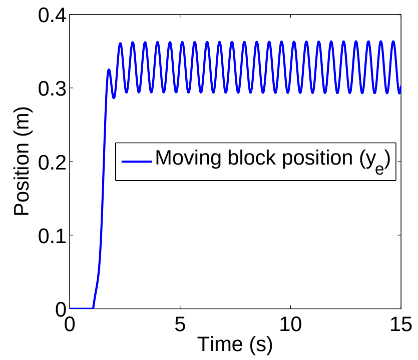

(a) POSITION VS TIME WITH DELAYS $p = p_0$

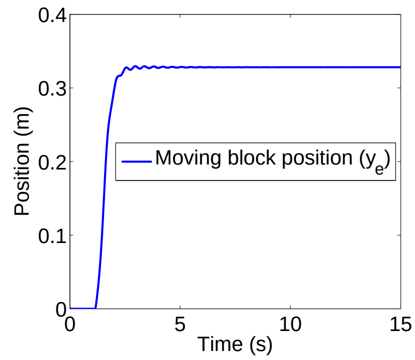

(b) POSITION VS TIME WITH DELAYS $p = p_1$

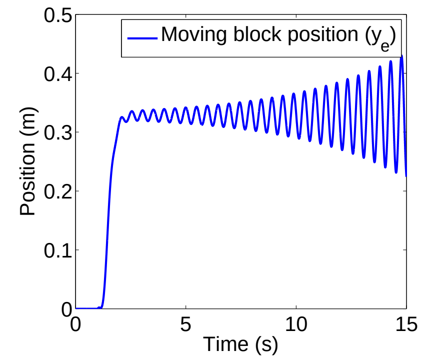

(c) POSITION VS TIME WITH DELAYS $p = p_2$

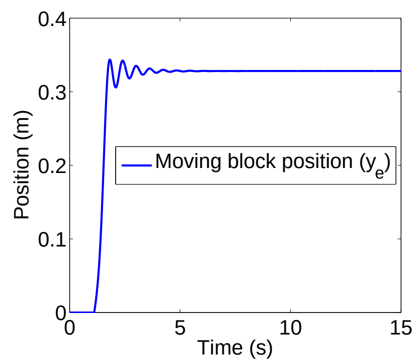

(d) POSITION VS TIME WITH DELAYS $p = p_3$

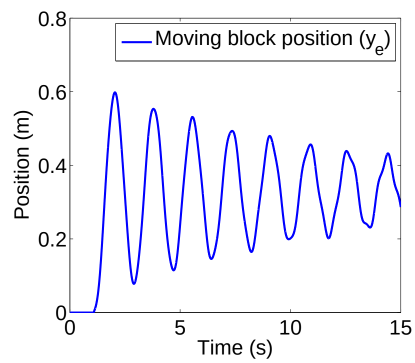

(e) POSITION VS TIME WITH DELAYS $p = p_4$

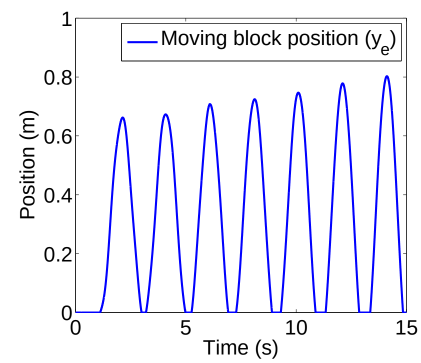

(f) POSITION VS TIME WITH DELAYS $p = p_5$

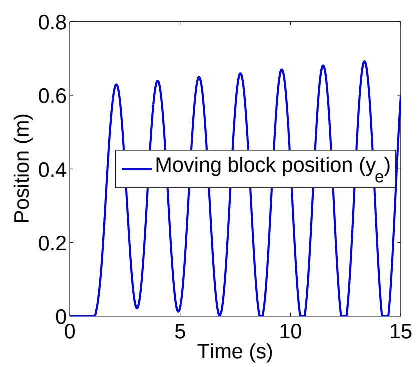

(g) POSITION VS TIME WITH DELAYS $p = p_6$

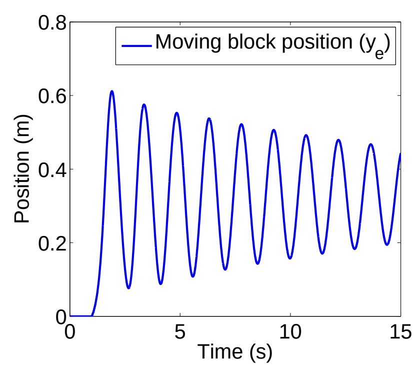

(h) POSITION VS TIME WITH DELAYS $p = p_7$

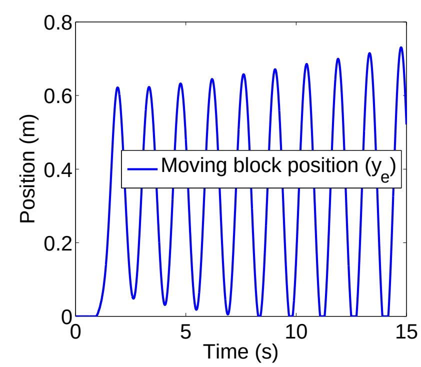

(i) POSITION VS TIME WITH DELAYS $p = p_8$

Figure 6. SIMULATION RESULTS

EXPERIMENTAL RESULTS

The prototype designed at the laboratory uses a computer with Windows XP operating system, which runs MATLAB-SIMULINK along with the WinCon software. This setup allows performing a real time experiment with the FAD. We have used a sampling time of 1 ms. The control parameters used for the experiments are $K_A = 125$, $K_d = 65\,\mathrm{kg\,s^{-1}}$ and $K_p = 45\,\mathrm{kg\,s^{-2}}$. Fig. 7 and Fig. 8 show the experimental results. It can be noted from Fig. 8 that the human operator is experiencing a load of $\approx 2\,\mathrm{N} \approx 204\,\mathrm{g}$ while lifting a mass of 24 kg.

Conclusion

In this paper we have proved the stability of the interaction of a human and a FAD. We have considered a general human operator model proposed in [12]. We have proved the stability in

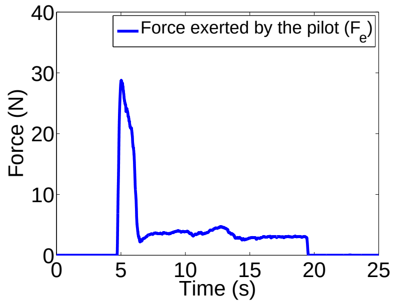

Figure 8. EXPERIMENTAL RESULT: FORCE VS TIME

the case of zero delays using the Routh-Hurwitz criterion. When the human model includes time-delays, we have also found an upper bound for the delays such that the stability is preserved.

It should be pointed out that the actual delays presented by any healthy human being are about four times smaller than the upper bound found for the delays in this study, beyond which instability will occur in the system. For this reason from a practical point of view we can consider our scheme to be robust enough against delays.

The numerical simulations presented show that if the delays are maintained below the upper bound found, the system is stable.

A real time experiment was conducted in a prototype. It was observed that the human machine interaction is stable and it is also observed that the damping introduced is sufficient enough to maintain the system without any oscillation. It is also observed that the operator is actually exerting a small fraction of the total force needed to lift the weight.

ACKNOWLEDGMENT

The authors would like to thank Gerardo Castro, and Jesús Meza, for their help in the electrical setup and Roberto Lagunes for his help with the mechanical setup.

REFERENCES

[1] Guizzo, E., and Goldstein, H., 2005. "The rise of the body bots [robotic exoskeletons]". *Spectrum, IEEE,* ***42***(10), pp. 50–56.

[2] Kim, W., Lee, S., Lee, H., Yu, S., Han, J., and Han, C., 2009. "Development of the heavy load transferring task oriented exoskeleton adapted by lower extremity using qausi-active joints". In ICCAS-SICE, 2009, IEEE, pp. 1353–1358.

[3] Snyder, T., and Kazerooni, H., 1996. "A novel material handling system". In 1996 IEEE International Conference on Robotics and Automation, 1996. Proceedings., Vol. 2, IEEE, pp. 1147–1152.

[4] Operation, S. M. H. P., 1969. Hardiman 1 prototype project. Tech. rep., General Electric Company, Schenectady, New York 12305, December.

[5] Kazerooni, H., 1988. "Human machine interaction via the transfer of power and information signals". *ASME Winter Annual Meeting*, DECEMBER.

[6] Kazerooni, H., 1990. "Human-robot interaction via the transfer of power and information signals". *IEEE Transactions on Systems, Man and Cybernetics,* ***20***(2), pp. 450–463.

[7] Lee, S., and Sankai, Y., 2002. "Power assist control for leg with hal-3 based on virtual torque and impedance adjustment". In 2002 IEEE International Conference on Systems, Man and Cybernetics, Vol. 4, IEEE, pp. 6–pp.

[8] Yamamoto, K., Hyodo, K., Ishii, M., and Matsuo, T., 2002. "Development of power assisting suit for assisting nurse labor". *JSME International Journal Series C,* ***45***(3), pp. 703–711.

[9] Kazerooni, H., 2006. "The Berkeley lower extremity exoskeleton". In Field and Service Robotics, Springer, pp. 9–15.

[10] Kong, K., and Tomizuka, M., 2009. "Control of exoskeletons inspired by fictitious gain in human model". *IEEE/ASME Transactions on Mechatronics,* ***14***(6), pp. 689–698.

[11] Merton, P., 1953. "Speculations on the servo-control of movement". In Ciba Foundation Symposium-The Spinal Cord, Wiley Online Library, pp. 247–260.

[12] McIntyre, J., and Bizzi, E., 1993. "Servo hypotheses for the biological control of movement". *Journal of Motor Behavior,* ***25***(3), pp. 193–202.

[13] Schweighofer, N., Arbib, M., and Kawato, M., 1998. "Role of the cerebellum in reaching movements in humans. i. distributed inverse dynamics control". *European Journal of Neuroscience,* ***10***(1), pp. 86–94.

[14] Schweighofer, N., Spoelstra, J., Arbib, M., and Kawato, M., 1998. "Role of the cerebellum in reaching movements in humans. ii. a neural model of the intermediate cerebellum". *European Journal of Neuroscience,* ***10***(1), pp. 95–105.

[15] Oshima, T., Fujikawa, T., Kameyama, O., and Kumamoto, M., 2000. "Robotic analyses of output force distribution developed by human limbs". In Robot and Human Interactive Communication, 2000. RO-MAN 2000. Proceedings. 9th IEEE International Workshop on, IEEE, pp. 229–234.

[16] Gadi, S. K., Lozano, R., Garrido, R., and Osorio, A., 2012. "Stability analysis and experiments for a force augmenting device". In 9th International Conference on Electrical Engineering, Computing Science and Automatic Control (CCE), 2012, pp. 1–6.

[17] Latash, M., and Gottlieb, G., 1991. "Reconstruction of shifting elbow joint compliant characteristics during fast

and slow movements". *Neuroscience,* ***43***(2-3), pp. 697–712.

[18] Olgac, N., and Sipahi, R., 2003. "The direct method for stability analysis of time delayed LTI systems". In American Control Conference, 2003. Proceedings of the 2003, Vol. 1, IEEE, pp. 869–874.

[19] Rekasius, Z., 1980. "A stability test for systems with delays". In Proceedings of the Joint Automatic Control Conference, San Francisco, CA, paper TP9-A.

[20] Pataky, T., Latash, M., and Zatsiorsky, V., 2005. "Viscoelastic response of the finger pad to incremental tangential displacements". *Journal of biomechanics,* ***38***(7), pp. 1441–1449.

[21] Michiels, W., and Niculescu, S., 2008. *Stability and Stabilization of Time-Delay Systems: An Eigenvalue-Based Approach*. Advances in Design and Control. Society for Industrial and Applied Mathematics.

[22] Neimark, J., 1949. "D-subdivisions and spaces of quasipolynomials". *Prikladnaya Matematika i Mekhanika,* ***13***, pp. 349–380.

Appendix: Remaining part of the stability proof

Simplifying b_1 from (22), we get

$$\begin{aligned} b_1 = &\Big[(BJ+G_vJK)(K_d+K_f)^2+(B^2M+J^2K_p+EJ^2K_A \\ &+G_v^2K^2M+2BG_vKM)(K_d+K_f)+(G_p+1)G_vK^2M^2 \\ &+EG_vKM^2l_a^2+B(G_p+1)KM^2+BEM^2l_a^2\Big]\Big/\Big[(B \\ &+G_vK)M+J(K_d+K_f)\Big]>0 \end{aligned} \tag{48}$$

Condition (23) can be simplified as

$$\begin{aligned} c_{1s} &:= b_1A_1-A_3A_0>0 \\ &= \Big[B^3EK_A(K_d+K_f)M+B^3(K_d+K_f)K_pM+B^2E^2K_AM^2l_a^2 \\ &\quad +3B^2EG_vKK_A(K_d+K_f)M+B^2EJK_A(K_d+K_f)^2 \\ &\quad +B^2E(K_d+K_f)^2Ml_a^2+B^2(G_p+1)K(K_d+K_f)^2M \\ &\quad +3B^2G_vK(K_d+K_f)K_pM+B^2J(K_d+K_f)^2K_p \\ &\quad +2BE^2G_vKK_AM^2l_a^2+3BEG_v^2K^2K_A(K_d+K_f)M \\ &\quad +2BEG_vJKK_A(K_d+K_f)^2+2BEG_vK(K_d+K_f)^2Ml_a^2 \\ &\quad +BEJ(K_d+K_f)^3l_a^2+2B(G_p+1)G_vK^2(K_d+K_f)^2M \\ &\quad +B(G_p+1)JK(K_d+K_f)^3+3BG_v^2K^2(K_d+K_f)K_pM \\ &\quad +2BG_vJK(K_d+K_f)^2K_p+E^2G_v^2K^2K_AM^2l_a^2 \\ &\quad +E^2J^2K_A(K_d+K_f)^2l_a^2+EG_v^3K^3K_A(K_d+K_f)M \\ &\quad +EG_v^2JK^2K_A(K_d+K_f)^2+EG_v^2K^2(K_d+K_f)^2Ml_a^2 \\ &\quad +EG_vJK(K_d+K_f)^3l_a^2+(G_p+1)G_v^2K^3(K_d+K_f)^2M \\ &\quad +(G_p+1)G_vJK^2(K_d+K_f)^3+G_v^3K^3(K_d+K_f)K_pM \\ &\quad +G_v^2JK^2(K_d+K_f)^2K_p+G_vK(K_d+K_f)\Big(-EMl_a^2+JK_p \\ &\quad +EJK_A-(G_p+1)KM\Big)^2+2E^2G_vJKK_A(K_d+K_f)Ml_a^2 \\ &\quad +B(K_d+K_f)\Big(-EMl_a^2+JK_p+EJK_A-(G_p+1)KM\Big)^2 \\ &\quad +2BE^2JK_A(K_d+K_f)Ml_a^2\Big]\Big/\Big[BM+J(K_d+K_f) \\ &\quad +G_vKM\Big]>0 \end{aligned} \tag{49}$$

Conditions (21), (48) and (49) are satisfied for all positive coefficients, so the polynomial is always stable considering no delays.